

Article

Energy Accumulation Characteristics and Induced Rockburst Mechanism of Roadway Surrounding Rock under Multiple Mining Disturbances: A Case Study

Zhenkai Ma ¹, Sheng Li ¹ and Xidong Zhao ^{2,*}

¹ School of Mining, Liaoning Technical University, Fuxin 123000, China; 471710042@stu.lntu.edu.cn (Z.M.); lisheng@lntu.edu.cn (S.L.)

² School of Mine Safety, North China Institute of Science and Technology, Langfang 065201, China

* Correspondence: 201701233zxd@ncist.edu.cn; Tel.: +86-136-9925-4895

Abstract: The source of energy release when rockburst occurs must be determined to understand the mechanisms underlying disaster formation and achieve accurate prevention and control. Although previous research has systematically investigated the energy source underlying rockburst from different perspectives, issues such as an unclear understanding of the energy accumulation state and inaccurate positioning of the energy release source remain to be resolved. In this study, the “1·17” major roof accident in the Danshuigou Mine was used as the background to evaluate and analyze the stress environment and energy accumulation characteristics of roadway surrounding rock under multiple mining disturbances, and the results showed that a super energy package occurs in the surrounding rock of the mining roadway. Subsequently, the evolution process of energy in this region and the mechanism of induced rockburst were elaborated. The results showed that the degree of stress concentration in the surrounding rock of the roadway will increase several times as the number of mining disturbances increases. Under the influence of multiple mining disturbances, the maximum principal stress peak of the surrounding rock of the roadway can reach 5–10 times the maximum principal stress value outside the mining-affected area. A large amount of elastic energy was accumulated in the rock surrounding the roadway, and super-high-density energy packages were formed locally. The maximum energy density value reached 50–185 times the value observed in areas outside the mining-affected zone. Thus, rockburst may be induced when the large amount of energy accumulated in the super energy package is suddenly and violently released; moreover, the degree of energy accumulation in the super energy package is likely closely related to the magnitude of rockburst. These results have important theoretical significance and application value for clarifying the mechanism of rockburst and improving the effectiveness of rockburst prediction and prevention.

Keywords: multiple mining disturbances; stress field; energy accumulation; super energy package; rockburst



Citation: Ma, Z.; Li, S.; Zhao, X. Energy Accumulation Characteristics and Induced Rockburst Mechanism of Roadway Surrounding Rock under Multiple Mining Disturbances: A Case Study. *Sustainability* **2023**, *15*, 9595. <https://doi.org/10.3390/su15129595>

Academic Editors: Fangtian Wang, Cun Zhang, Shiqi Liu and Erhu Bai

Received: 15 May 2023

Revised: 9 June 2023

Accepted: 12 June 2023

Published: 15 June 2023



Copyright: © 2023 by the authors. Licensee MDPI, Basel, Switzerland. This article is an open access article distributed under the terms and conditions of the Creative Commons Attribution (CC BY) license (<https://creativecommons.org/licenses/by/4.0/>).

1. Introduction

Rockburst is one of the main dynamic disasters threatening the safety and efficient production of coal mines [1,2]. Over the past five years, eight rockburst accidents have occurred in China, resulting in 48 deaths and more than 100 injuries. With the increase in mining scale, mining depth, and mining intensity, a more serious rockburst disaster development trend is expected to occur [3–5].

Rockburst is a dynamic failure phenomenon caused by the sudden release of elastic energy accumulated in coal and rock mass when the mechanical system of coal and rock reaches the strength limit [6–8]. Coal mining under different geological and mining technology conditions leads to diverse manifestations of rockburst, and although the specific mechanisms differ [9–11], a consensus has been reached in academic and engineering circles that rockburst is driven by energy [12–15].

The formation of rockburst is closely related to the elastic strain energy accumulated in the surrounding rock [16–18]. According to energy theory [19], rockburst occurs when the energy released by the coal-surrounding rock system is greater than the energy consumed when its mechanical equilibrium state is destroyed. This theory was previously used to explain the cause of rockburst from the perspective of energy conversion. Li et al. [20] first deduced the calculation formula of the energy distribution of an elastic foundation beam and analyzed the distribution law of energy accumulation and energy release before and after the fracture of the hard roof plate in front of the work face. Zhou et al. [21,22] studied the coupling effect of elliptical cavities and cracks on tunnel stability under static and dynamic loads. Guo et al. [23] applied elastoplastic mechanics to deduce the stress distribution formula and releasable strain energy concentration of roadway surrounding rock. Hao et al. [24] investigated a rockburst accident in the Chengshan Coal Mine by studying the influence of the upper goaf, roof strength, and excavation time on the energy distribution in front of the working face. Tan et al. [25] deduced the calculation method of kinetic energy generated in a coal body due to mining and proposed an evaluation index of the kinetic energy of rockburst risk. Chen et al. [26] explored the accumulation horizon of energy that causes rockburst in a coal–rock system, deduced the pre-peak energy distribution formula of coal–rock combinations, and studied the failure characteristics, mechanical properties, and energy accumulation law of the combination through tests. The integral volumetric measures of damage–dangerous volumes where stresses, strains, or energy surpass their limiting values are long and well known in the works on tribo-fatigue for systems simultaneously working in the conditions of fatigue, friction, wear, and thermal loads [27–29]. Sherbakov et al. [30] conducted computer modeling of stress–strain state and volumetric damageability in the neighborhood of a mine roadway and calculated volumetric damageability through the model of a deformed solid body with dangerous volume.

Previous research has systematically investigated the energy source underlying rockburst from different perspectives; however, the energy accumulation state is poorly understood, and a method of accurately locating the energy release source has not been developed. These issues remain to be resolved.

Based on the “1·17” major roof accident in the Danshuigou Mine, this study examined and analyzed the stress environment and energy accumulation characteristics of the roadway surrounding rock under the influence of multiple mining disturbances, and expounded the evolution process of the surrounding rock energy of the mining roadway and the mechanism of inducing rockburst. The results can be used as an important theoretical basis for determining the size and location of the energy source of rockburst. They also have certain engineering significance and reference value for further understanding the incubation and development process of rockburst and improving the monitoring and prevention efficiency of rockburst disasters.

2. Project Background

2.1. Project Overview

The Danshuigou Coal Mine is located in Xiaopingyi Township, north of Shuocheng District, Shuozhou City, Shanxi Province, China. The minable coal seams of the Danshuigou Coal Mine are coal seams 4⁻¹, 4⁻², 8, 9, and 11. The first-level coal seams 4⁻¹ and 4⁻² are jointly arranged, and the second-level coal seams 8, 9, and 11 are jointly arranged. The 4203 fully mechanized working face is located to the north of the main roadway in coal seam 4, the 4202 goaf is located to the east, and the lower part of the 4202 goaf corresponds to the 9202 goaf of coal seam 9. The strike length of working face 4203 is 1091 m, the dip length is 215 m, the average thickness of the coal seam is 5.68 m, and the dip angle of the coal seam is 2–14°, with an average of 5°. The working face adopts the long-wall coal mining method, the coal mining process is comprehensive mechanized mining, while the full-caving method is used to manage the roof. The direct roof and main roof of the working face are medium-coarse sandstone and mudstone, which present undeveloped

fissures. The thickness of the direct roof is 5.95 m, which belongs to the Class I stable roof category, and the thickness of the main roof is 3.97–9.04 m. The direct bottom and old bottom of the working face are mudstone and fine sandstone, respectively, which present undeveloped fissures. The thicknesses of the direct and old bottom are 3.91–9.35 m and 5.88 m, respectively.

The 4203 haulage roadway is excavated along the floor of coal seam 4 with a rectangular cross section. The roof support is a combination of support by bolt, anchor cable, steel belt, and metal diamond mesh. In the mining process of the 4203 working face, due to the coal roof of the haulage roadway, roof separation and roadway floor heave have occurred during mining. To ensure normal mining, some areas need to carry out roadway expansion operations, such as the expansion and repair of roadway sides, excavation and leveling of roadway floor. A single column with a steel cantilever beam is used to strengthen the support.

On 17 January 2017, a major roof accident occurred in the 4203 haulage roadway. The abnormal ground pressure phenomenon revealed by the accident was the first occurrence in this coal mine. The specific accident location and on-site excavation engineering layout are shown in Figure 1.

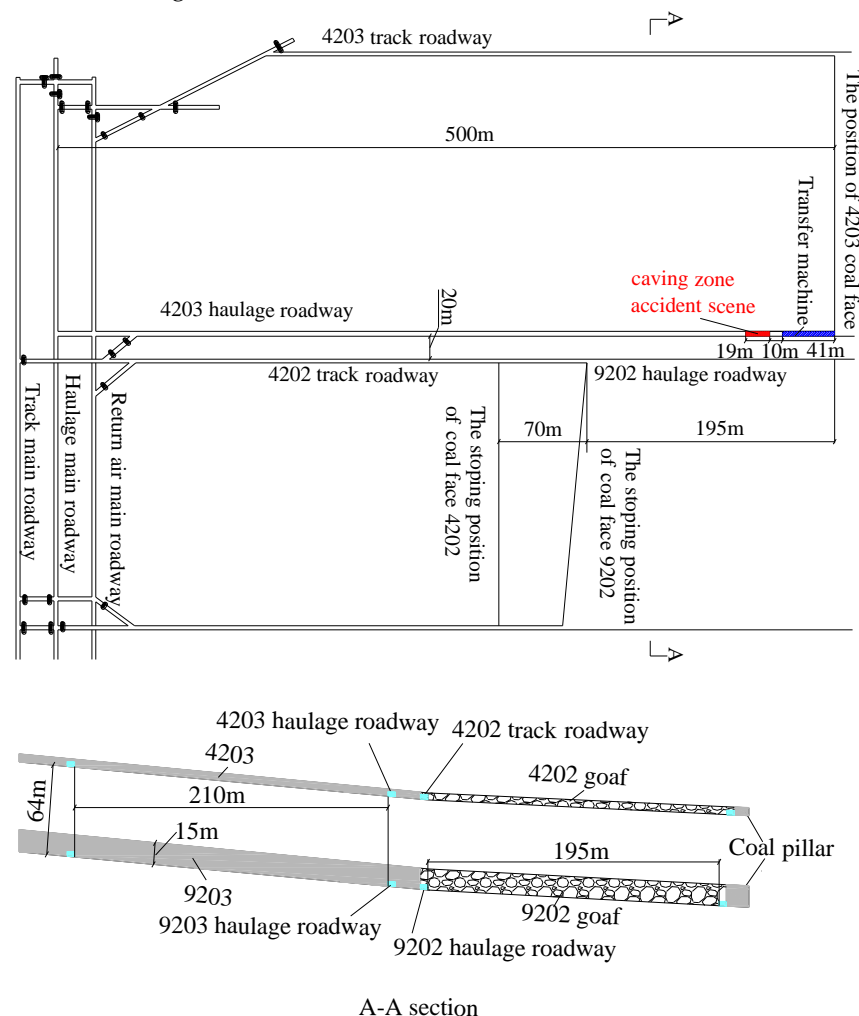


Figure 1. Schematic diagram of the accident location and surrounding mining layout of the 4203 working face haulage roadway.

2.2. Failure Characteristics of the Accident Roadway

After a major roof accident occurred in the 4203 haulage roadway, the roadway presented obvious sectional damage characteristics and typical dynamic damage characteristics as follows.

- (1) The accident roadway showed obvious characteristics of sectional damage. The 4203 haulage roadway is divided into five sections from the end of the working face outwards. As shown in Figure 1, the surrounding rock of the roadway within a range of 0–41 m in front of the working face was severely damaged (length 41 m). The transfer machine head was inclined, with one side close to the roof and the other side located 350 mm away from the roof, as shown in Figure 2. The roof with a range of 41–51 m in front of the working face was basically intact (length 10 m). The 51–70 m section in front of the working face presented evidence of the impact roof collapse (length 19 m), and its height of 2.0–2.5 m reached the direct roof. Most of the anchor rods on the side were exposed, the coal side was collapsed. The 70–200 m section in front of the working face was the damaged section outside the roof falling area, with 70–115 m being more severe. The roof and sides appeared to have a net pocket, and the floor bulge was severe. The normal rock pressure manifestation section was located 200 m away from the front of the working face, and the roadway surrounding rock was basically intact.
- (2) The accident roadway had typical dynamic damage characteristics. Some single hydraulic props were bent at 0–41 m in front of the working face. Within the 19-m-long roof fall and wall collapse section, more than 30 sets of roof bolts were broken, accounting for nearly 30% of the total number of bolts, most of them were broken without necking, and all 19 anchor cables were pulled apart, which is evidently different from the breaking and failure characteristics of bolts and anchor cables in ordinary roof fall accidents, as shown in Figure 3. According to the data provided by the Center of Seismological Network of Shanxi Province, the SHC Shenchi Station (~42 km away), PIG Pianguan Station (~83 km away), KEL Kelan Station (~80 km away), and L1410 Yuanping Station (~78 km away) all experienced obvious “earthquake anomalies” when the accident occurred.



Figure 2. Photo of the tilting of the end transfer machine on the working face.



Figure 3. Photo of the anchor bolt (cable) breaking.

3. Establishment of a Numerical Model

3.1. Numerical Calculation Model

Based on the actual data for the Danshuigou Mine, a numerical calculation model was developed (length \times width \times height = 1000 m \times 530 m \times 170 m), where the horizontal displacement of the x and y axis boundary was fixed, and the vertical displacement of the lower boundary of the z axis was fixed, as shown in Figure 4. A compensation load of 8 MPa was applied to the upper boundary to simulate the unit weight of the rock layer above the model, and the initial stress field determined from the field stress data was applied. The Mohr–Coulomb constitutive model and the Mohr–Coulomb failure criterion were applied for calculation. The physical and mechanical parameters of the rock mass are shown in Table 1.

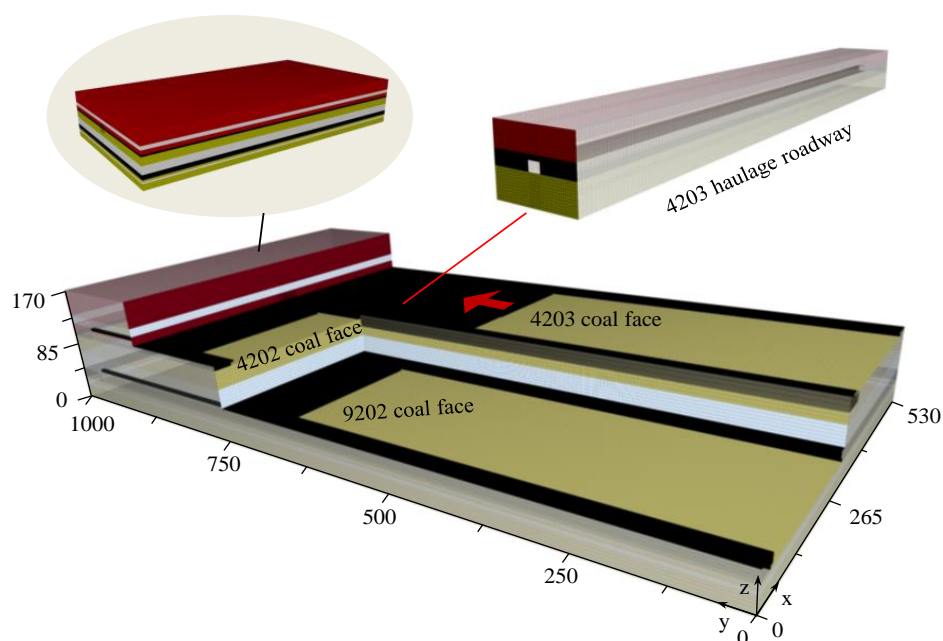


Figure 4. Numerical calculation model.

Table 1. Mechanical parameters of the stratified rock mass in the model.

Stratum	Density/(kg/m ³)	Bulk Modulus/GPa	Shear Modulus/GPa	Cohesion/MPa	Friction Angle/°
mudstone	2480	9.97	7.35	4.4	32
medium-coarse sandstone	2630	18.7	22.0	6.6	36
coal seam 4 ⁻²	1380	4.91	2.01	3.7	32
fine sandstone	2540	2.7	1.6	4.0	35
mudstone	2480	9.97	7.35	4.6	32
coal seam 9	1380	4.91	2.01	3.8	32
mudstone	2480	9.97	7.35	4.2	32
fine sandstone	2540	2.7	1.6	4.0	35

For the research of the relationship among the stress environment and energy evolution observed in the surrounding rock of the 4203 haulage roadway and the impact roof fall accident, the width and height of the 4203 haulage roadway were set to 5 m \times 4 m, respectively, in the numerical calculation model. Considering the influence of roadway excavation on the stress change of the surrounding rock, the section size of the surrounding rock of the 4203 haulage roadway was set to 35 m \times 26 m (width \times height); that is, the ratio of width direction to roadway width was 7, and the height direction was 6.5. This study assumed that the rock mass outside the mining surrounding rock was not affected by roadway excavation.

3.2. Calculation Schemes

Based on the mining layout of the working face when the 4203 haulage roadway roof fall accident occurred in the Danshuigou Coal Mine, four calculation schemes are proposed, as shown in Figure 5. Scheme I: considering the influence of single mining disturbance, only the 4203 working face will be mined to 490 m. Scheme II: considering the influence of double mining disturbances, the 4202 working face is first mined to the stopping position of 755 m, and then the 4203 working face is mined to 490 m. Scheme III: considering the influence of double mining disturbances, the 9202 working face is first mined to the stopping position of 685 m, and the 4203 working face is mined to 490 m. Scheme IV: considering the influence of triple mining disturbances, the 4202 and 9202 faces are mined to the stopping position of 755 m and 685 m, then the 4203 face is mined to 490 m.

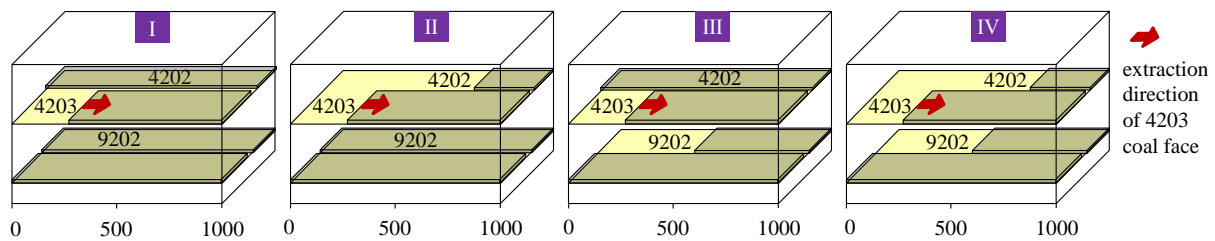


Figure 5. Mining layout schemes of the working face.

4. Stress Environment Characteristics of the Roadway Surrounding Rock

4.1. Vector Characteristics of the Mining Roadway Surrounding Rock Stress State

Figure 6 shows the calculation results of the vector distribution of the main stress field of the 4203 haulage roadway at 20 m in front of the working face under four different calculation schemes. According to the results, under the influence of double mining disturbances, the size of the main stress field significantly increased compared with that of a single working face; moreover, the direction of the main stress field changed significantly. However, under the influence of triple mining disturbances, the maximum principal stress field of the roadway surrounding rock increased several times compared with the influence of double mining disturbances, while that of the local area increased nearly 10 times. In addition, the uneven distribution of the principal stress field in the roadway section increased significantly, especially in the roof of the roadway, where the stress concentration was higher.

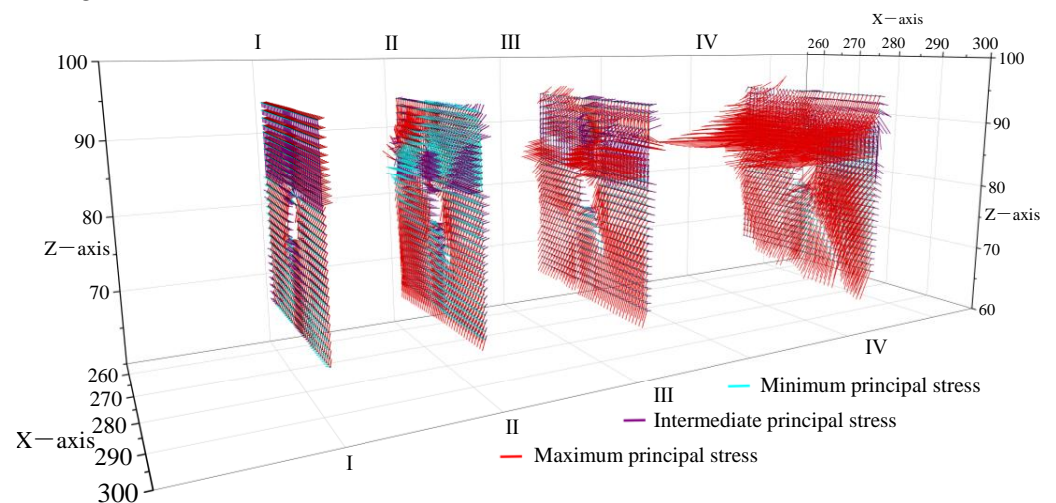


Figure 6. Vector distribution of the principal stress field of the roadway surrounding rock section under different mining schemes.

4.2. Distribution Characteristics of the Surrounding Rock Stress Field of Mining Roadway

According to the above calculation results, the maximum principal stress value in the area where the depth of the roof surrounding rock was 4 m was extracted along the axial direction of the roadway, and the center line of the roadway roof was used as a benchmark. The results are shown in Figure 7. Under the influence of mining disturbance at different working faces, the distribution of the maximum principal stress field was significantly different. Among them, the maximum principal stress under the influence of triple mining disturbances was far greater than the calculation results under the influence of single or double mining disturbances. From the peak value of the maximum principal stress field, the calculation result under the influence of triple mining disturbances was 3–5 times the peak value under the influence of double mining disturbances, 6.6 times the peak value under the influence of a single mining disturbance, and 7.3 times the peak value outside the area of a mining disturbance in front of the working face. Among them, a comparison of Schemes II and III showed that the 9202 working face had a greater impact on the peak value of the principal stress than the 4202 working face, and the stress increase range under the influence of triple mining disturbances could reach 300 m in front of the working face.

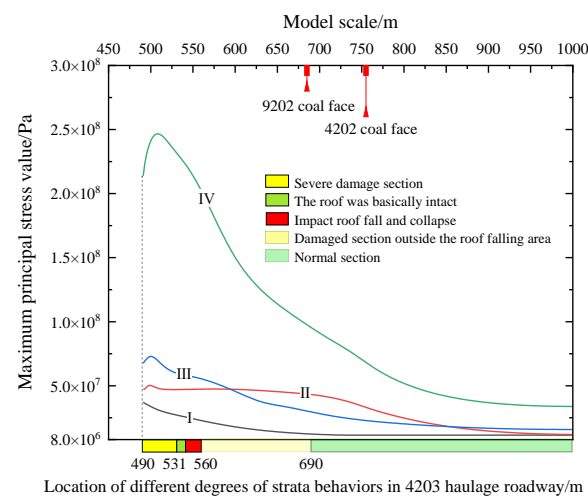


Figure 7. Stress distribution of the roadway surrounding rock in different mining schemes.

Figure 8 shows the calculation results based on Scheme IV when working face 4203 is located at different mining locations. According to the calculation results, in the mining process of working face 4203, the peak value of the maximum principal stress was 5–10 times that of outside the mining-affected area and centered on the stopping position of working face 9202. Before this position, the peak value of the maximum principal stress continuously increased, while after this position, the peak value gradually decreased, the distribution of the maximum principal stress no longer appeared in the stress rise area, and the peak value was directly located near the working face.

The results shown in Figures 7 and 8 were used to compare the damage area of the accident roadway with the distribution of the stress field. The mining stress field of the 4203 haulage roadway moved dynamically during the advance of the 4203 working face. With the approach to the stopping position of the 9202 working face, the stress concentration degree gradually increased. When the working face advanced to the accident location, the continuously migrating and increasing dynamic high stress acted on the 4203 haulage roadway, thereby inducing rockburst. The impact stress caused instantaneous destruction of the roof and floor of nearly 200 m of roadway and the two sides of the coal body, simultaneously broke a large number of bolts and cables in the local roadway, and led to local roof fall and wall collapse. Among them, the rockburst induced by multiple mining stresses was the direct cause of roof fall and wall collapse.

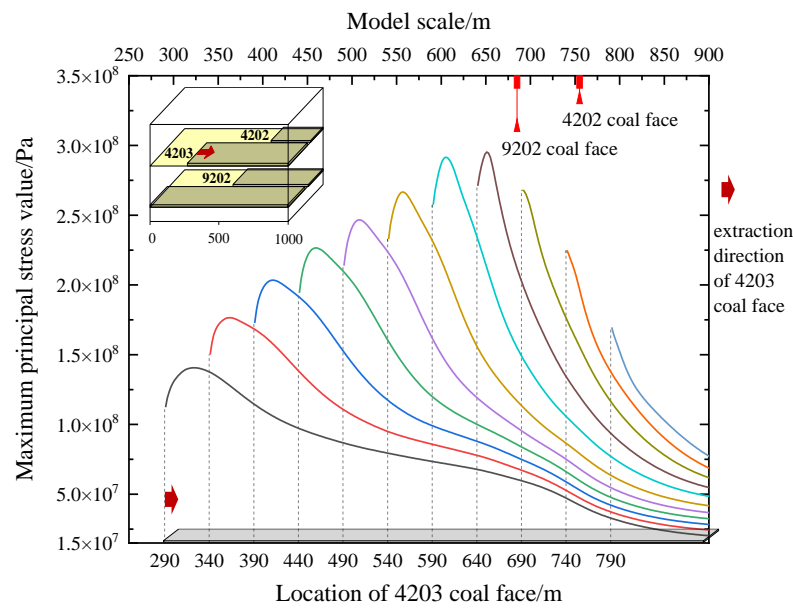


Figure 8. Stress distribution of the roadway surrounding rock in different mining positions.

5. Energy Accumulation Characteristics of the Roadway Surrounding Rock

When a rock mass undergoes elastic deformation due to external forces, energy accumulates inside the mass because of work by external forces. If the energy loss is not considered, then all work done by external forces acting slowly in the elastic range will be accumulated in the rock mass in the form of strain energy [31]. Therefore, when the surrounding rock of the roadway is affected by multiple mining disturbances, the rock mass under strong mining stress may accumulate huge amounts of elastic energy. In the elastic state, for the mining roadway surrounding rock in a certain area (expressed in Ω), the energy stored in any unit of its space can be expressed as follows [32,33]:

$$f(x, y, z) = \frac{1}{2E_i} \left[\sigma_{1i}^2 + \sigma_{2i}^2 + \sigma_{3i}^2 - 2\mu_i(\sigma_{1i}\sigma_{2i} + \sigma_{2i}\sigma_{3i} + \sigma_{1i}\sigma_{3i}) \right] * \Delta V_i \quad (1)$$

where E_i is the elastic modulus of the unit; σ_{1i} , σ_{2i} , and σ_{3i} are the maximum, intermediate, and minimum principal stresses of the unit, respectively; μ_i is the Poisson ratio of the unit; and ΔV_i is the unit volume.

As a certain plastic zone range usually forms around the roadway surrounding rock (denoted by Ω_p) and its micro unit is still considered to be in the elastic state, the elastic strain energy density of this area can be calculated by Equation (1) (at this time, the elastic modulus and Poisson ratio are the values under the plastic state). Under this state, the energy accumulated in the surrounding rock of the mining roadway can be expressed by Equation (2):

$$U = \iiint_{\Omega} f(x, y, z) dV = \iiint_{\Omega_e} f(x, y, z) dV_e + \iiint_{\Omega_p} f(x, y, z) dV_p \quad (2)$$

where Ω_e represents the rock mass area in an elastic state, i.e., $\Omega_e = \Omega - \Omega_p$.

5.1. Energy Accumulation Characteristics of the Roadway Surrounding Rock

According to the above, within the 4203 haulage roadway surrounding rock section along the axial direction of the roadway, the roadway surrounding rock with a length of 2 m was considered as the calculation unit to calculate the energy accumulated in the mining roadway surrounding rock within this range. Figure 9 shows the calculated energy accumulation distribution within the surrounding rock of the 4203 haulage roadway under the four different calculation schemes. According to the results, the energy accumulation

value of the roadway surrounding rock under the influence of triple mining disturbances was far greater than that under single or double mining disturbances. The peak value of energy accumulation of the roadway surrounding rock under the influence of triple mining disturbances can reach 1.53×10^9 J, which is equivalent to the energy of 364.3 kg TNT (4.2×10^6 J/kg), 4.6 and 3.1 times the peak value of accumulated energy under the influence of mining disturbances in the double working faces 4203 + 4202 and 4203 + 9202, respectively, 24 times the peak value of accumulated energy under the influence of mining disturbances in the single working face, and 72 times the value of accumulated energy outside the mining influence area in front of the working face. Under the influence of triple mining disturbances, the distribution characteristics of the accumulated energy in the roadway surrounding rock are noticeable and show a trend of initially increasing, then decreasing, and then tending to be flat. The range of the energy increase zone can reach 300 m away from the front of the working face. Under the influence of single or double mining disturbances, the zone of increasing energy distribution is small or disappears, and the range of the zone of increasing energy is relatively small.

The calculation results based on Scheme IV when working face 4203 is located at different mining locations are shown in Figure 10. According to the results, under the influence of triple mining disturbances, the accumulated energy of the surrounding rock of the 4203 haulage roadway was at a high level, and the peak value of the accumulated energy of the roadway surrounding rock was 15–73 times the accumulated energy value outside the mining influence area in front of the working face, which gradually increased while approaching the mining stopping position of the 9202 working face, the accumulated energy reached the maximum value at the 590 m position and then gradually decreased. Therefore, from the perspective of the evolution process of the accumulated energy of the roadway surrounding rock with the mining of the working face, the stopping position of the 9202 and 4202 working faces significantly affected the change in its peak value.

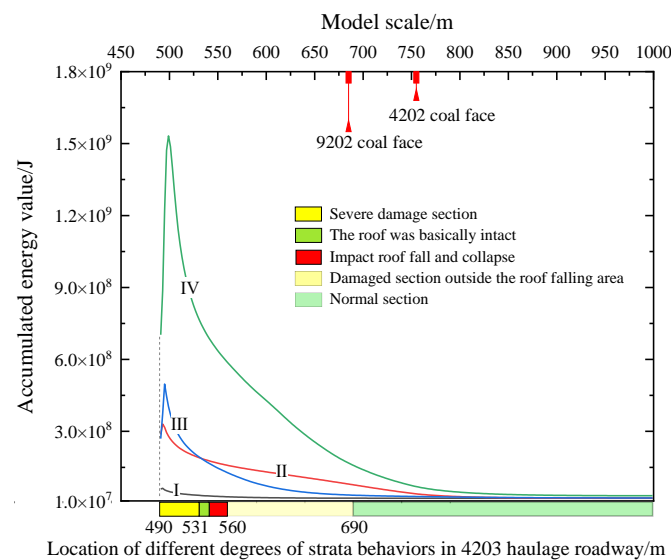


Figure 9. Distribution of accumulated energy of the roadway surrounding rock under different mining schemes.

According to the above analysis and the results shown in Figures 9 and 10, the energy value accumulated in the surrounding rock caused by mining in the 4203 haulage roadway moved and increased with the dynamic migration and gradual increase in the concentration of the mining stress field during the advance of the 4203 working face. When the working face advanced to the accident location, the large amount of energy accumulated in the roadway surrounding rock provided the energy basis for the occurrence of rockburst.

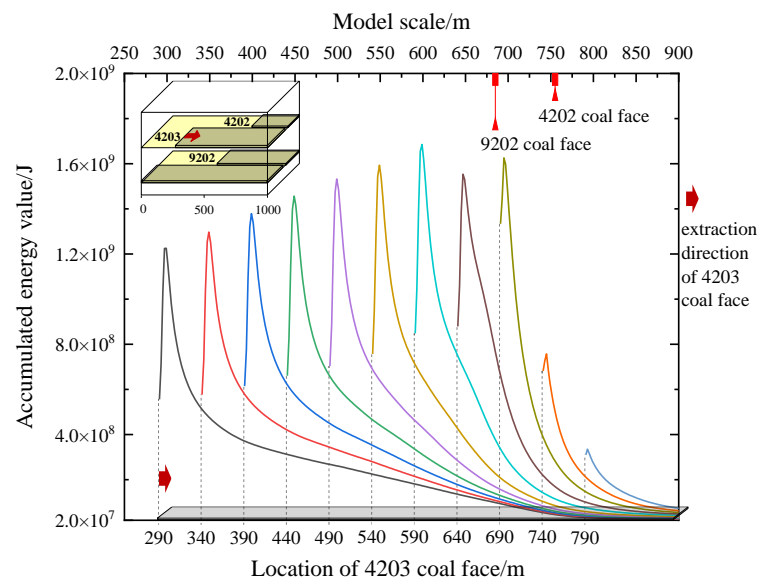


Figure 10. Distribution of accumulated energy of the roadway surrounding rock under different mining positions.

5.2. Super Energy Package of the Roadway Surrounding Rock and Its Evolution Characteristics

5.2.1. Super Energy Package and Its Connotation

The energy density distribution of the roadway section in Figure 6 was calculated, and the results are shown in Figure 11. Under strong triple mining stress, the stress concentration degree of the roadway surrounding rock increased several times. Due to the regional concentration of the mining stress distribution, a super-high-density energy accumulation area was locally formed in the roadway surrounding rock, and the maximum energy density value in the section can reach 35 times under the influence of the mining of a single working face.

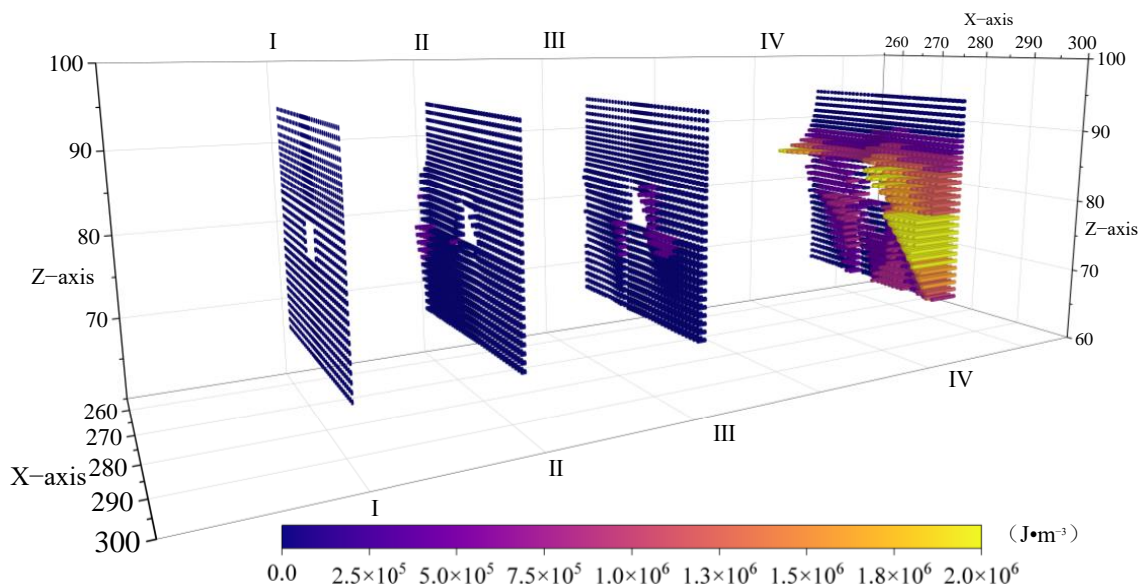


Figure 11. Comparison of the energy density distribution of the roadway surrounding rock section under different mining schemes.

When working face 4203 was located in different mining positions, according to the energy accumulation area of the roadway surrounding rock, along the axial direction of the roadway, i.e., the Y direction, take the section at X = 288 m, and the energy density distribu-

tion was calculated, as shown in Figure 12. In the mining process of the 4203 working face, under continuous increases of mining stress concentration, the energy accumulated in the 4203 haulage roadway increased, and the distribution of the energy field also underwent cumulative adjustment. Simultaneously, combined with the calculation results in Figure 11, in the mining process of working face 4203, a super-high-density energy package occurred in the roadway surrounding rock, which is termed as the super energy package in this study. When a certain energy density value is determined as the boundary of the super energy package, the energy density value of the rock mass within the boundary of the super energy package increases in multiples, and a region containing the maximum energy density is formed in the center, known as the energy nucleus, the center of the energy nucleus is the region where the maximum energy density is located in the super energy package. The scope, shape and internal stored energy of the super energy package changes significantly with the change of the position of the 4203 working face.

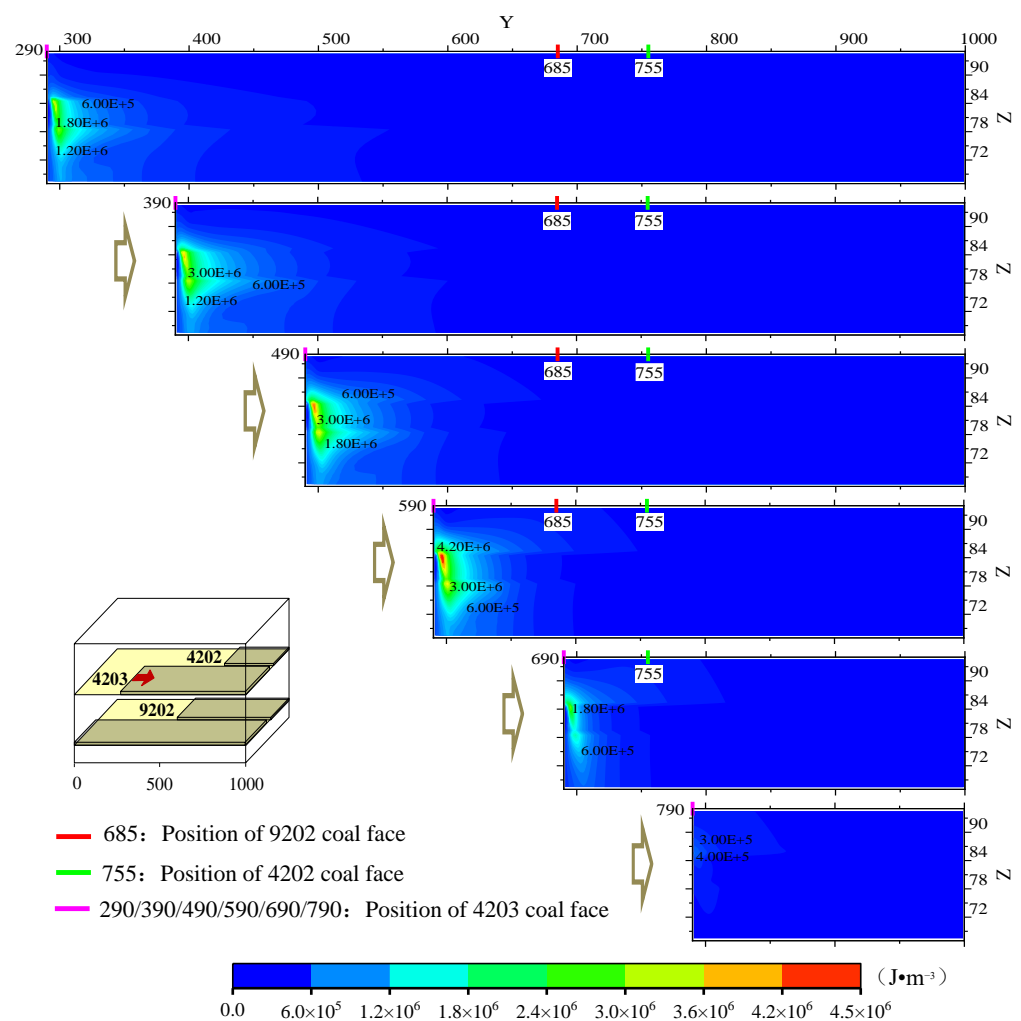


Figure 12. Energy density distribution of the 4203 transport roadway surrounding rock when the 4203 working face is located at different mining positions.

5.2.2. Evolution Characteristics of Super Energy Package

To characterize the evolution characteristics of the super energy package with the change of the mining position of the 4203 working face, the maximum energy density value was extracted in the surrounding rock section of the 4203 haulage roadway, that is, the maximum energy density within a certain section of the surrounding rock of the roadway, and the maximum energy density distribution curve of the surrounding rock in different sections was formed along the axial direction of the roadway, as shown in Figure 13. Before the stopping

position of the 9202 working face, the distribution of the maximum energy density presented a “double peak” feature of “increase → decrease → increase → decrease → flat.” At this time, the maximum energy density in the super energy package was the maximum value of the maximum energy density distribution curve. After the stopping position of the 9202 working face, it transformed into a “single peak” that followed the form “increase → decrease → flat”.

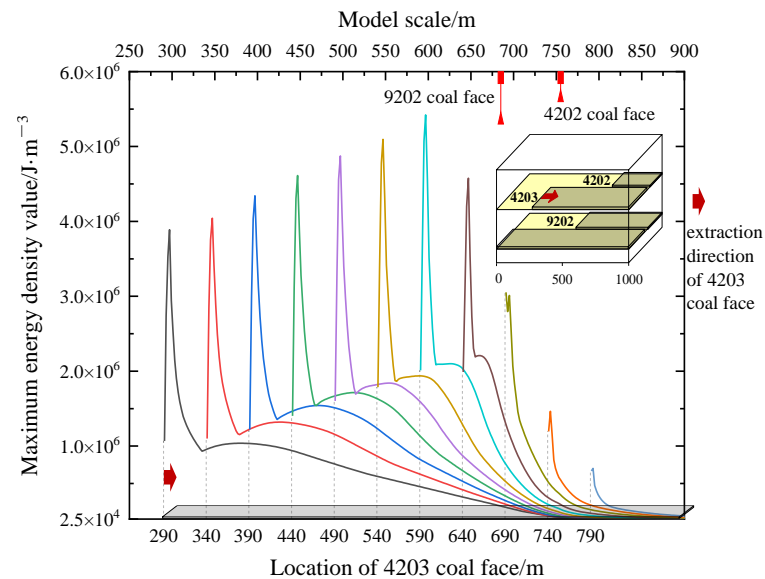


Figure 13. Distribution curve of the maximum energy density.

Figure 14 shows the calculation results of the maximum energy density distribution eigenvalue. Here, nuclear is the maximum energy density in the super energy package, and the center position of nuclear is the distance between the maximum energy density in the super energy package and the working face. With the continuous approaching of the working face 4203 and the stopping position of working face 9202, the maximum energy density in the super energy package gradually increased and reached the maximum values at 590 m. In this process, the central part of nuclear stabilizes at 7 m in front of the working face. Afterwards, as the 4203 working face continued to advance, the maximum energy density in the super energy package began to gradually decrease, and the distance between the center of the energy nuclear and the working face was also gradually approaching.

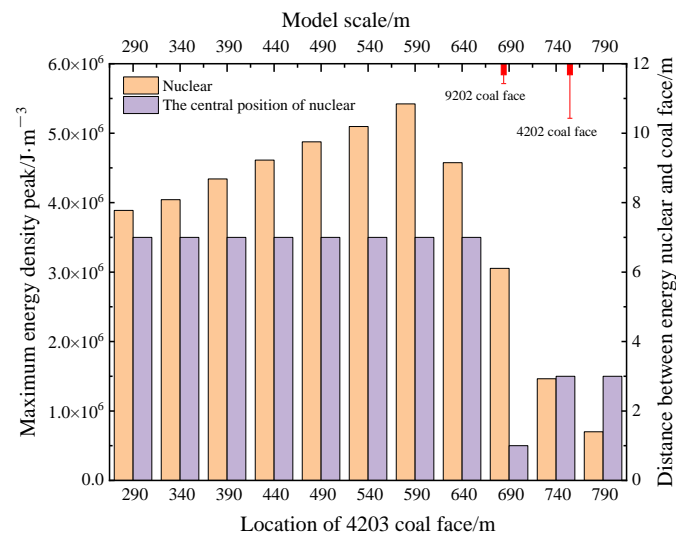


Figure 14. Distribution characteristic values of the maximum energy density.

Under the influence of triple mining disturbances, the maximum energy density value of the super energy package in the surrounding rock of the 4203 haulage roadway was at a high level. The accumulation degree of energy in the super energy package changes significantly with the position of the working face, and the maximum energy density value inside the super energy package can reach values 50–185 times that outside the mining-affected area. Considering the mining of the working face to be 490 m (i.e., the position of the 4203 working face when the accident occurred) as an example, the maximum value of the energy density in the energy package was $4.87 \times 10^6 \text{ J/m}^3$, which was 166 times that of the maximum energy density outside the mining-affected area in front of the working face. When the huge energy accumulated in the super energy package reached a certain limit, it may become the main energy source underlying rockburst catastrophe accidents.

6. Discussion

In the process of the deformation and destruction of rocks, energy input, accumulation, dissipation, and release occurs [34,35]. Consider the mining roadway within a certain range in front of the coal face as a relatively closed system (4203 haulage roadway with a certain range, as mentioned earlier), that is, the surrounding rock system of a mining roadway. The surrounding rock system of the mining roadway likely also experiences energy input, energy accumulation, energy dissipation, and energy release during working face mining. The spatiotemporal evolution of these four aspects of energy is closely related to rockburst disasters induced by energy.

6.1. Energy Evolution Process of the Surrounding Rock of Mining Roadway

(1) Energy input

External energy inputs mainly refer to the work done by external forces. For the surrounding rock system of the mining roadway, the external force can be considered mining stress that is constantly moving with the advance of the working face during the mining process. Increased mining stress acts on the surrounding rock system of the mining roadway, and the external force impacts the system and also inputs external energy. In addition, the external force includes the dynamic load caused by rock mass fracture of the outer roof of the surrounding rock system of the mining roadway, fault activation, earthquakes, and other mining engineering disturbances.

(2) Energy accumulation

For the surrounding rock system of a mining roadway, part of the external input energy is accumulated in the surrounding rock of the roadway in the form of elastic deformation energy, which is reversible and can be released when the increased mining stress is unloaded. When energy is input from an external source, the surrounding rock system of the mining roadway accumulates energy continuously, and the distribution of the energy field forms a super-high-density energy package due to the local adjustment of the stress state of the mining surrounding rock. Under different mining conditions, the degree of energy accumulation in the super energy package varies greatly. When the huge energy accumulated in the super energy package reaches a certain limit, it may become the main energy source of rockburst catastrophe accidents.

(3) Energy dissipation

When an external force acts to input energy into the surrounding rock system of the mining roadway, if the stress in the surrounding rock exceeds its elastic limit, the surrounding rock will produce plastic deformation. Due to the irreversibility of plastic deformation, this is a process of energy dissipation. Simultaneously, the energy input from the outside not only leads to the further development of initial damage (cracks and holes) in the roadway surrounding rock, but also produces new cracks and holes in the surrounding rock; that is, part of the energy is dissipated in the form of irreversible damage energy. As the energy input increases, the amount of energy transformed into plastic deformation energy and damage energy becomes larger. In the surrounding rock system of the mining

roadway, it is specifically manifested in the expansion of the plastic zone of the surrounding rock and the increase of the degree of fragmentation of surrounding rock.

(4) Energy release

Energy release mainly refers to the energy released by the surrounding rock system of the mining roadway to the outside world (mainly refers to the roadway space and the rock mass outside the system). The intensity of energy release in unit time can be graded according to the magnitude of the earthquake. When the energy accumulated in the surrounding rock system is released evenly and slowly, it is mainly manifested in the form of general ground pressure manifestations, such as roof subsidence, wall bulge, and floor heave. When the energy accumulated in the surrounding rock system is released violently in a short time, it is mainly manifested in the form of dynamic destruction of the surrounding rock, such as rock mass ejection, surrounding rock vibration, and roadway roof fall, simultaneously, accompanied by the sound of surrounding rock fracture, the intensity of the released energy is positively related to its destructiveness [36,37], which can severely destroy mechanical equipment and support components in the roadway space and cause casualties.

6.2. Mechanism of Rockburst Induced by Energy Accumulation in the Surrounding Rock of Mining Roadway

In the mining process of the working face, when dynamic changes of the surrounding rock stress field in the mining space occur and the stress field of the surrounding rock system of the mining roadway is in a specific stress state, the corresponding energy field has a specific energy state corresponding to the state [38]. Under certain mining conditions, the energy of the surrounding rock system of the mining roadway is continuously accumulated and forms a super energy package with a very high energy density value. Subsequently, the sudden and violent release of the huge energy accumulated in the super energy package can induce rockburst. In this process, the formation of the super energy package and the degree of its energy accumulation are important factors that induce rockburst. The huge energy accumulated in the super energy package will become the main energy source of the dynamic disaster accident. As shown in the previous research results, under the influence of triple mining disturbances, the mining surrounding rock system in a certain area of the 4203 haulage roadway experienced four processes of energy input, accumulation, dissipation, and release during the advancing process of the working face. With the continuous input of external energy, the energy in the mining surrounding rock system continues to accumulate, and the energy accumulation degree in the super energy package also continues to increase. When the working face is pushed to the accident location, under the action of a trigger event, the huge energy accumulated in the super energy package will be released violently in a short time, thus triggering an impact roof fall accident.

The results of this study indicate that further theoretical exploration is required to determine how to prevent energy in the rock mass from accumulating at a local height, release the accumulated energy smoothly, and accurately predict and monitor the location and degree of rockburst during coal mining operations.

7. Conclusions

- (1) The stress environment characteristics of the roadway surrounding rock under the influence of multiple mining disturbances were studied and analyzed. The degree of stress concentration in the surrounding rock of the roadway will increase several times as the number of mining disturbances increases. The stress concentration degree of the roadway roof surrounding rock and the uneven degree of the stress field distribution are relatively higher, and the peak maximum principal stress can reach 5–10 times that outside the mining-affected area. During the mining process of the working face, as the distance from the stopping position of the adjacent working face decreases, the stress concentration degree of the roadway surrounding rock continues to increase during its dynamic migration.

- (2) Under the influence of multiple mining disturbances, a large amount of elastic energy is accumulated in the roadway surrounding rock and a super-high-density energy package is formed in the roadway surrounding rock. The maximum energy density value in the super energy package can reach 50–185 times that of outside the mining-affected area. The degree of energy accumulation in the super energy package will change significantly with the change of the location of the working face. When the huge energy accumulated in the super energy package reaches a certain limit, it may become the main energy source of the dynamic disaster accident. This relationship can be used as an important theoretical basis for determining the size and location of the energy source of rockburst.
- (3) The evolution process of the surrounding rock energy of a mining roadway and the mechanism of induced rockburst are expounded. Under the influence of multiple mining disturbances, the energy of the surrounding rock system of the mining roadway is continuously accumulated and forms a super energy package with a very high energy density value. When the huge energy accumulated in the super energy package is suddenly and violently released, it can cause dynamic destruction of the surrounding rock, such as rock mass ejection, surrounding rock vibration, and roadway roof fall, which are accompanied by the sound of surrounding rock fracture. The degree of energy accumulation in the super energy package is closely related to the magnitude of rockburst.

Author Contributions: Conceptualization, Z.M. and X.Z.; methodology, S.L.; software, Z.M.; validation, Z.M. and X.Z.; formal analysis, Z.M.; investigation, Z.M. and X.Z.; resources, S.L.; data curation, Z.M. and X.Z.; writing—original draft preparation, Z.M.; writing—review and editing, X.Z.; supervision, S.L.; project administration, X.Z.; funding acquisition, X.Z. All authors have read and agreed to the published version of the manuscript.

Funding: This research was funded by the National Natural Science Foundation of China, grant number 51804117.

Institutional Review Board Statement: Not applicable.

Informed Consent Statement: Not applicable.

Data Availability Statement: The data used to support the findings of this study are available from the corresponding author upon request.

Acknowledgments: The authors would like to thank the peer reviewers and editors for their valuable comments and suggestions, which have greatly improved the manuscript presentation.

Conflicts of Interest: The authors declare no conflict of interest.

References

1. Pan, Y.S.; Song, Y.M.; Zhu, C.L.; Ren, H.; Xu, H.L. Localization method of coal rock deformation for rock burst prediction. *J. China Coal Soc.* **2023**, *48*, 185–198.
2. Pan, J.F.; Kang, H.P.; Yan, Y.D.; Ma, X.H.; Ma, W.T.; Lu, C.; Lv, D.Z.; Xu, G.; Feng, M.H.; Xia, Y.X.; et al. The method mechanism and application of preventing rock burst by artificial liberation layer of roof. *J. China Coal Soc.* **2023**, *48*, 636–648.
3. Zhang, H.W.; Li, S.; Han, J.; Song, W.H.; Lan, T.W.; Rong, H.; Fu, X.; Yang, Z.H. Geo-dynamic division and its application in study of rock burst. *Coal Sci. Technol.* **2023**, *51*, 191–202.
4. Jang, F.X.; Zhang, X.; Zhu, S.T. Discussion on key problems in prevention and control system of coal mine rock burst. *Coal Sci. Technol.* **2023**, *51*, 203–213.
5. Yang, Y.; Cao, A.; Liu, Y.; Bai, X.; Yan, Z.; Wang, S.; Wang, C. Understanding the Mechanism of Strong Mining Tremors near the Goaf Area of Longwall Mining: A Case Study. *Appl. Sci.* **2023**, *13*, 5364. [[CrossRef](#)]
6. Song, D.Z. Research on Rockburst Evolutionary Process and Energy Dissipation Characteristics. Ph.D. Thesis, China University of Mining and Technology, Xuzhou, China, 2012.
7. Zhu, X.J.; Pan, Y.S.; Li, Q.; Wang, A.W.; Wang, K.X.; Chen, J.J. Softening zone energy extremum criterion and experimental study of roadway rock burst. *J. China Univ. Min. Technol.* **2021**, *50*, 975–982.
8. Wang, G.; Li, G.; Dou, L.; Mu, Z.; Gong, S.; Cai, W. Applicability of energy-absorbing support system for rockburst prevention in underground roadways. *Int. J. Rock Mech. Min.* **2020**, *132*, 104396. [[CrossRef](#)]

9. Xu, C.; Fu, Q.; Cui, X.; Wang, K.; Zhao, Y.; Cai, Y. Apparent-Depth Effects of the Dynamic Failure of Thick Hard Rock Strata on the Underlying Coal Mass During Underground Mining. *Rock Mech. Rock Eng.* **2019**, *52*, 1565–1576. [\[CrossRef\]](#)
10. Li, X.L.; Chen, S.J.; Wang, E.Y.; Li, Z.H. Rockburst mechanism in coal rock with structural surface and the microseismic (MS) and electromagnetic radiation (EMR) response. *Eng. Fail. Anal.* **2021**, *124*, 105396. [\[CrossRef\]](#)
11. Zhu, S.T.; Feng, Y.; Jiang, F.X. Determination of abutment pressure in coal mines with extremely thick alluvium stratum: A typical kind of rockburst mines in China. *Rock Mech. Rock Eng.* **2016**, *49*, 1943–1952. [\[CrossRef\]](#)
12. Shi, T.W.; Pan, Y.S.; Wang, A.W.; Dai, L.P. Classification of rock burst in coal mine based on energy storage and release bodies. *J. China Coal Soc.* **2020**, *45*, 524–532.
13. Xue, C.C.; Cao, A.Y.; Guo, W.H.; Liu, Y.Q.; Wen, Y.Y.; Hu, Y.; Li, X.W. Energy evolution law and rock burst mechanism of deep thick seams with large inclination. *J. Min. Saf Eng.* **2021**, *38*, 876–885.
14. Zhang, J.W.; Dong, X.K.; Cai, H.T.; Yang, L.; Zhao, S.K.; Wang, Q.; Lv, Y.L.; Jia, L.L.; Bai, J.J.; Zheng, B.; et al. Structure evolution and rockbursts prevention in multi-face mining in geological anomaly area. *Coal Sci. Technol.* **2023**, *51*, 95–105. [\[CrossRef\]](#)
15. Wang, S.W.; Ju, W.J.; Pan, J.F.; Lu, C. Mechanism of energy partition evolution of excavation roadway rockburst in coal seam under tectonic stress field. *J. China Coal Soc.* **2019**, *44*, 2000–2010.
16. Konicek, P.; Waclawik, P. Stress changes and seismicity monitoring of hard coal longwall mining in high rockburst risk areas. *Tunn. Undergr. Space Technol.* **2018**, *81*, 237–251. [\[CrossRef\]](#)
17. Jiang, L.S.; Kong, P.; Zhang, P.P.; Shu, J.M.; Wang, Q.B.; Chen, L.J.; Wu, Q.L. Dynamic analysis of the rock burst potential of a longwall panel intersecting with a fault. *Rock Mech. Rock Eng.* **2020**, *53*, 1737–1754. [\[CrossRef\]](#)
18. Ma, N.J.; Guo, X.F.; Zhao, Z.Q.; Zhao, X.D.; Liu, H.T. Occurrence mechanisms and judging criterion on circular tunnel butterfly rock burst in homogeneous medium. *J. China Coal Soc.* **2016**, *41*, 2679–2688.
19. Lippmann, H. *Mechanical Considerations of Bumps in Coal Mines, Rockbursts and Seismicity in Mines*; Fairhurst, E., Ed.; Balkema: Rotterdam, The Netherlands, 1990; pp. 279–284.
20. Li, X.Y.; Ma, N.J.; Zhong, Y.P.; Gao, Q.C. Storage and release regular of elastic energy distribution in tight roof fracturing. *Chin. J. Rock Mech. Eng.* **2007**, *26*, 2786–2793.
21. Zhou, L.; Chen, J.X.; Zhou, C.L.; Zhu, Z.M.; Dong, Y.Q.; Wang, H.B. Study on failure behaviors of mixed-mode cracks under static and dynamic loads. *Geomech. Eng.* **2022**, *29*, 567–582.
22. Zhou, L.; Ma, L.J.; Zhu, Z.M.; Dong, Y.Q.; Huang, J.W.; Cui, S.H. Study of the coupling effect of elliptical cavities and cracks on tunnel stability under dynamic loads. *Theor. Appl. Fract. Mec.* **2022**, *121*, 103502. [\[CrossRef\]](#)
23. Guo, H.J. Research on the Energy Evolution Laws of Surrounding Rock Unloading and the Rockburst Mechanism in Solid Coal Roadway Excavation. Ph.D. Thesis, China University of Mining and Technology, Xuzhou, China, 2019.
24. Hao, F.K.; Li, H.T.; Zhou, K.; Wang, X. Study on Numerical Simulation of Main Control Factors for Energy Distribution of Mine Pressure Bump. *Coal Sci. Technol.* **2014**, *42*, 31–34.
25. Tan, Y.L.; Wang, Z.H.; Liu, X.S.; Wang, C.W. Estimation of dynamic energy induced by coal mining and evaluation of burst risk. *J. China Coal Soc.* **2021**, *46*, 123–131.
26. Chen, G.B.; Zhang, J.W.; He, Y.L.; Zhang, G.H.; Li, T. Derivation of pre-peak energy distribution formula and energy accumulation tests of coal-rock combined body. *Rock Soil Mech.* **2022**, *43*, 130–143+154.
27. Shcherbakov, S.S. Modeling of the damaged state by the finite-element method on simultaneous action of contact and noncontact loads. *J. Eng. Phys. Thermophys.* **2012**, *85*, 472–477. [\[CrossRef\]](#)
28. Shcherbakov, S.S. Spatial stress-strain state of tribofatigue system in roll–shaft contact zone. *Strength Mater.* **2013**, *45*, 35–43. [\[CrossRef\]](#)
29. Zhuravkov, M.A.; Sherbakov, S.S.; Krupoderov, A.V. Modeling of volumetric damage of multielement clamp-knife-base tribofatigue system. *ZAMM Z. Angew. Math. Mech.* **2017**, *97*, 60–69. [\[CrossRef\]](#)
30. Sherbakov, S.S.; Shemet, L.A.; Nasan, A.A. Computer modeling of volumetric damageability in the mine roadway neighbourhood. *Dokl. BGUIR* **2020**, *18*, 47–54. [\[CrossRef\]](#)
31. Qian, M.G.; Shi, P.W.; Xu, J.L. *Mine Pressure and Strata Control*, 2nd ed.; China University of Mining and Technology Press: Xuzhou, China, 2010; pp. 46–48.
32. Du, F.; Ma, J.; Guo, X.; Wang, T.; Dong, X.; Li, J.; He, S.; Nuerjuma, D. Rockburst mechanism and the law of energy accumulation and release in mining roadway: A case study. *Int. J. Coal Sci. Technol.* **2022**, *9*, 67. [\[CrossRef\]](#)
33. Hao, Z.; Guo, L.F.; Zhao, X.D.; Chen, G.X.; Zhang, G.H. Analysis of burst failure energy characteristics of mining roadway surrounding rock. *J. China Coal Soc.* **2020**, *45*, 3995–4005.
34. Zhang, Z.Z. Energy Evolution Mechanism during Rock Deformation and Failure. Ph.D. Thesis, China University of Mining and Technology, Xuzhou, China, 2013.
35. Bieniawski, Z.T.; Denkhaus, H.G.; Vogler, U.W. Failure of fractured rock. *Int. J. Rock Mech. Min. Sci.* **1969**, *6*, 323–330, IN29–IN32, 331–341. [\[CrossRef\]](#)
36. Qi, Q.X.; Li, Y.Z.; Zhao, S.K.; Pan, P.Z.; Wei, X.Z. Discussion on the mechanism and control of coal bump among mine group. *J. China Coal Soc.* **2019**, *44*, 141–150.

37. Holub, K.; Rusajova, J.; Holecko, J. Particle velocity generated by rockburst during exploitation of the longwall and its impact on the workings. *Int. J. Rock Mech. Min. Sci.* **2011**, *48*, 942–949. [[CrossRef](#)]
38. Liu, X.S.; Tan, Y.L.; Ning, J.G.; Tian, C.L.; Tian, Z.W. Energy criterion of abutment pressure induced strain-mode rockburst. *Rock Soil Mech.* **2016**, *37*, 2929–2936.

Disclaimer/Publisher’s Note: The statements, opinions and data contained in all publications are solely those of the individual author(s) and contributor(s) and not of MDPI and/or the editor(s). MDPI and/or the editor(s) disclaim responsibility for any injury to people or property resulting from any ideas, methods, instructions or products referred to in the content.